

# Optimal Threshold Estimation using Grey Wolf Optimization for EMD-DTCWT Based ECG Denoising

Deepak H. A., T. Vijayakumar

**Abstract:** The noise reduction in the ECG has been focused for research in recent years, since desired reduction allows a better signal pre-processing, and allows to extract from it the maximum amount of efficient and meaningful information. This paper proposes an adaptive threshold technique using Empirical Mode Decomposition (EMD) and Dual-Tree Complex Wavelet Transform (DTCWT) for ECG signal denoising. Initially the data driven EMD technique is applied to get the IMFS and these IMFS further passed through DTCWT for filtration. To accomplish the better adaptive filtering process the optimal threshold is further calculated based on Grey Wolf Optimization (GWO). The performance evaluation is achieved on MIT-BIH database.

**Keywords:** Cross Correlation, DTCWT, DWT, ECG, EEG, EMG, EMD, GWO, IMF, MAE, MSE, PSNR, SNR

## I. INTRODUCTION

The devices used in medical monitoring for biomedical signal processing are very sensitive in nature. Every medical diagnosis requires very accurate results. The medical monitoring equipment namely ECG, EMG and EEG are generally used in the diagnosis of patient accurate health diagnosis but getting the accurate results seems to be more complicated in every biomedical signal recording while the patient is diagnosed.

Currently, there are different professionals involved in biomedical research and electro-medicine such as: doctors, biologists, laboratory technicians, etc. who makes use of data obtained from electronic instruments, which is sometimes the only way to evaluate patients. Therefore, there must be a correct processing and examination of the acquired data with a focus on correct signal of the instruments and the appropriate information. In the particular case of cardiology, it seeks to detect cardiovascular diseases through non-invasive methods that avoid the minimum risk for the patient and in turn deliver the greatest amount of information to analyze the signal, the electrocardiogram is widely used tests in the modern day medical diagnosis since it meets required characteristics.

Cardiovascular illness is the main source of death around the world. These clutters are because of issues in coronary conduit (artery), cerebrovascular disease and intrinsic heart maladies [1].

To identify the wellbeing states of the heart it is a key symptomatic instrument utilized. It notes the charged action

of heart amid various periods of the cardiovascular cycle. The importance of the electrocardiographic signal (ECG) since the interpretation of a heaps of cardiac ailments is well known, both through visual inspection and through automatic inspection techniques [2].

The ECG signal is subject to a series of disturbances caused by the patient's movements or breathing, his muscular electrical activity, the inappropriate positioning of the electrodes, interference with the electrical network, etc. All these undesirable phenomena lead to the degradation of the quality of the recorded ECG signal and make its automatic processing difficult. Therefore, preliminary signal processing is highly necessary in most cases. Given the peculiarities of the field, the quality of such a preprocessing must be impeccable: it must consider the elimination of disturbing influences, while faithfully keeping the essential characteristics of the useful waves that make up the signal. These characteristics (among which we find the form, the duration, the spectrum) will be used later to extract the parameters which "decide" the classification, therefore their least degradation can affect the automatic "verdict", i.e. the classification of the patient. This clearly explains the importance of the quality of denoising [3] [4] [5].

In recent years, new techniques based on wavelet transform have become popular in the context of signal denoising [6] [7] [8]. Indeed, this transform has the remarkable property of "concentrating" most of the energy of the useful signal in a reduced number of high energy coefficients in the "transformed" domain. On the other hand, the coefficients representing the image of noise in the domain of the wavelet transform will be numerous, but of low energy.

The electrical activity generated by various cells get decreased with the biomedical signals due to the Hilbert-Huang transform which is generally based on empirical mode decomposition [8] [9] [10]. It allows the decomposition of non-stationary signals into a series of modes or IMF (Intrinsic Mode Function) in an iterative manner [11].

The presence of noise in the signal of interest will lead to contamination of each of the modes by a more or less large fraction of this noise. The reading of the spectral content and the statistical characteristics of each of the modes, obtained after EMD applied to white noise, made it possible to define a behavior model allowing the determination of the informative content of each of the IMFs [10]. This model was widespread by Flandrin et al. in the case of fractional Gaussian noise [12] [13].

**Revised Manuscript Received on March 10, 2020.**

**Deepak H. A.**, Research Scholar, Department of E&C, SJBIT, Bangalore, Affiliated to VTU, Belagavi, India. E-mail: [deepakgowdal@gmail.com](mailto:deepakgowdal@gmail.com)

**Dr. T. Vijayakumar**, Professor, Department of E&C, SJBIT, Bangalore, Affiliated to VTU, Belagavi, India. E-mail: [tvijakumar@sjbit.edu.in](mailto:tvijakumar@sjbit.edu.in)

These models can be utilized for a denoising application or to suppress the trend of the signal of interest. These models assume that the first IMF contains only a fraction of the noise. The energy estimate of the first IMF is then used systematically to customize the model and adapt it to the characteristics of the noise corrupting the signal. An error in the approximation of the noise level can therefore degrade the performance of the algorithm. One of these sources of error can be the mixing of modes. The mixing of modes corresponds to the time alternation on the same IMF of several components of the signal of interest [12]. In our application, the mode mixing will mainly concern the high frequency part of the noise and the first natural high frequency component of the signal. This mixing phenomenon will therefore lead to an overestimation of the noise level contained in the first IMF.

An algorithm to avoid the mixing of modes has been proposed in [12]. This algorithm is conversely dedicated to EMD analysis of signals containing purely sinusoidal components. The performance of this algorithm on signals with more complex non-stationary components, as commonly encountered in the field of mechanics or biomedical engineering, is not guaranteed. Many authors have therefore developed specific algorithms dedicated to their signal of interest. The algorithm presented here makes no assumption about the nature of the components of the signal of interest and is therefore a general alternative to preexisting algorithms.

After briefly recalling the classic algorithm for selecting the relevant modes, we will propose an improvement of this algorithm by the prior use of a stationarity test on the first IMF, allowing a more robust estimation of the statistical thresholds to be applied to each of the IMF. The performance of our algorithm will then be evaluated on purely synthetic signals, and also on real signals from mechanics and biomedical.

This paper presents a framework of EMD-DTCWT based ECG signal denoising using a metaheuristic approach; Grey Wolf Optimization. Section two describes the implementation of proposed approach. Results are presented in section three trailed by the conclusive remarks in the section four.

## II. PROPOSED METHODOLOGY

Methodology to be adapted in the proposed work is elaborated in this chapter. Figure 1 shows the flow of proposed research work.

- Initially Empirical mode decomposition (EMD) of ECG signal is performed to get the intrinsic mode functions (IMFs).
- DTCWT is performed on IMFs for prediction of noisy peaks and separating them from signal.
- Removal of noise in DTCWT is performed by soft thresholding method (GWO). Then power spectral subtraction is performed and finally filtered IMFs are summed up to get the reconstructed signal.

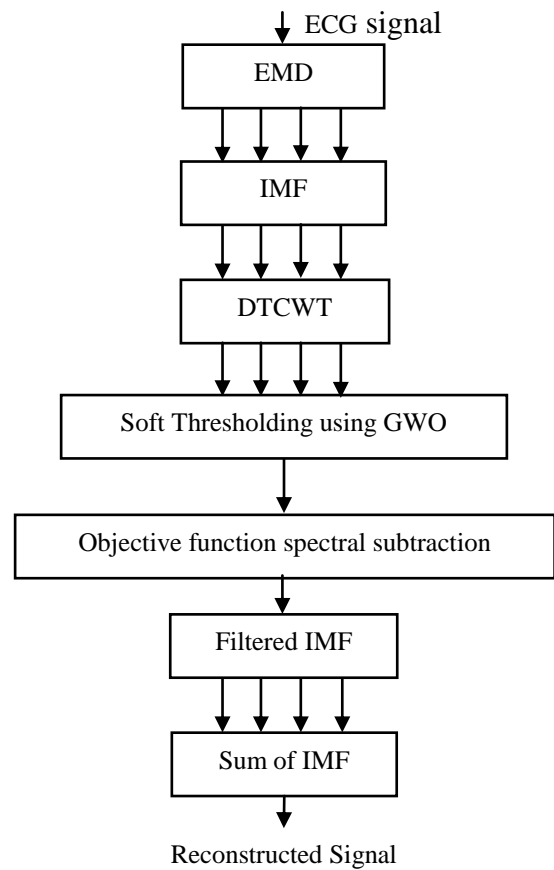


Figure 1: Flow diagram for proposed research work

### A. Empirical Mode Decomposition (EMD)

The initial point of the EMD is the treatment of the oscillations at a very local level which corresponds to the observation of the signal  $x(t)$  between two extrema of the same nature, either two minima or two maxima [14].

Taking the case where the extrema correspond to two minima; between these two ends, one can define two local parts:

- A high frequency local part called local detail: it resembles to the oscillation existing between the two minima and taking into account the maximum existing between them,
- A local part of low frequency called local tendency,

The application of this principle on the whole of the signal  $x(t)$  makes it possible to decompose it into two parts; the signals describing the high frequencies denoted by  $d(t)$  and the signals describing the low frequencies denoted by  $m(t)$ . dimensionally The signal  $x(t)$  is then expressed by:

$$x(t) = d(t) + m(t) \quad (1)$$

We iterate over the low frequency component until we can define all the modes existing in the signal. These modes are represented by functions modulated in amplitude and frequency, called IMFs.

#### 1. Description of the Intrinsic Mode Function (IMF)

An IMF is a simple oscillating function modulated in amplitude and frequency. It must meet the following two conditions [9]:

1. The average IMF value is zero.
2. Throughout the entire length of the IMF, the difference between the number of extrema and the number of zero crossings must be equal to 0 or 1. This means that between a minimum and a maximum, the IMF must go through zero. For example, Figure 2 illustrates a signal that does not correspond to an IMF. Indeed, between the maximum (*Max1*) and the minimum (*Min1*), the signal does not pass through a zero.

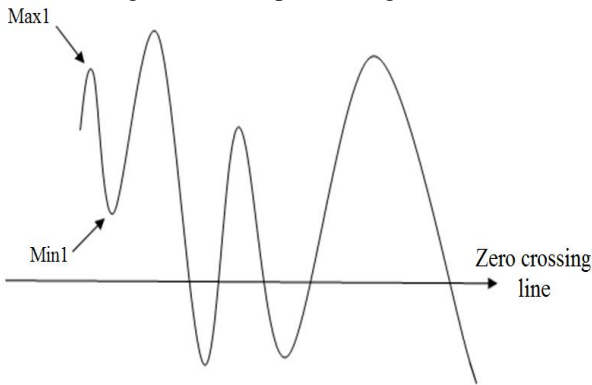


Figure 2: Example of a signal that does not correspond to an IMF [9]

## 2. Description of the Method

The method of the EMD will follow the subsequent stages:

1. Extraction of the extrema (maxima and minima).
2. Once the extrema are acknowledged, all the local maxima are associated by a cubic line defining the high envelope  $e_{high}$ , the same process is continued for the local minima in order to produce the lower envelope  $e_{low}$ ; these two envelopes will thus cover the entire signal.
3. The next step is the calculation of the average of the two high and low envelopes according to the following formulation:

$$m(t) = \frac{e_{high}(t) + e_{low}(t)}{2} \quad (2)$$

4. The first component, denoted by  $h(t)$ , is obtained by the following relation:

$$h(t) = x(t) - m(t) \quad (3)$$

5. The signal  $h(t)$  will correspond to an IMF only if it fulfills the conditions of the IMF. If not,  $h(t)$  is considered a new signal for the next iteration  $x(t) \leftarrow h(t)$ . This iterative and sequential process is called the sifting process.

6. Once the first IMF has been identified, iterates over the residue. Represented as:

$$r(t) = x(t) - IMF(t) \quad (3)$$

7. The decomposition is interrupted only when the residue has an extrema,

The different steps described above are shown in the flowchart in Figure 3.

## 3. The Algorithm for EMD

IMF function = EMD( $x$ )

1 initialization:

Put:

$$IMF = [];$$

$k = 1;$   
 $r_k = x;$   
 2 Screening process: extract the  $k^{th}$  IMF  
 2.1 initialization:  
 Put  
 $j = 1;$   
 $h_j = r_k;$

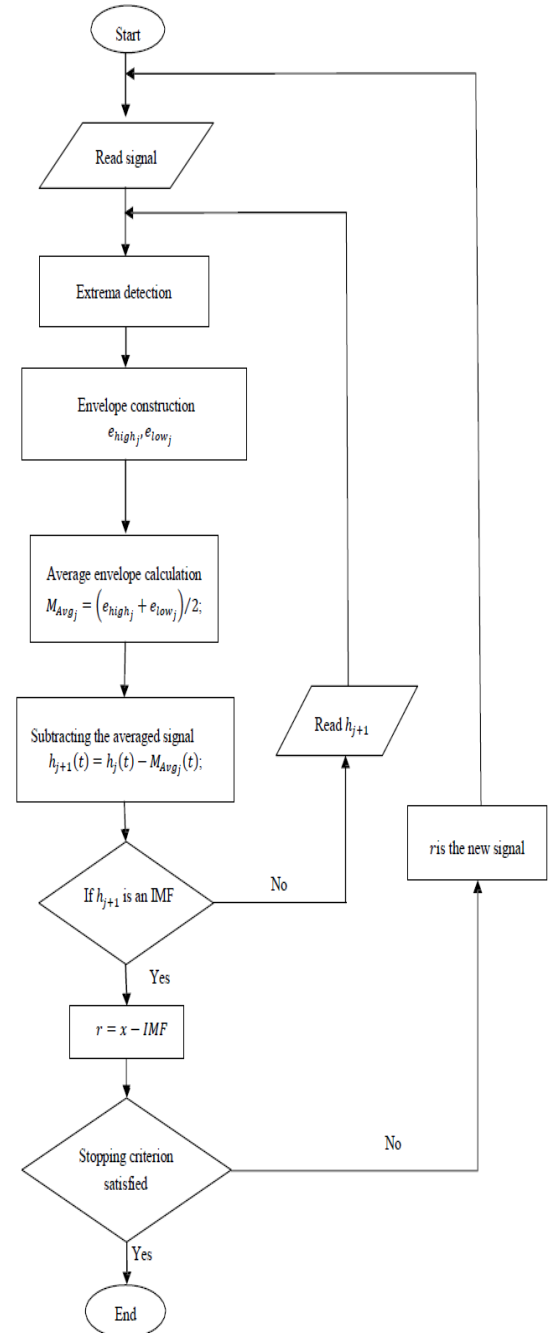


Figure 3: The flowchart describing the empirical mode decomposition.

2.2 Identification of local extrema (maximums and minimums) in  $h_j$ ;

2.3 Construction of high envelope ( $e_{highj}$ ) from the interpolation of points corresponding to local maxima;

2.4 Construction of low envelope ( $e_{low_j}$ ) from the interpolation of the points corresponding to the local minima;

2.5 Calculating the average of the high and low envelopes:

$$M_{Avg_j} = (e_{high_j} + e_{low_j})/2;$$

2.6 Subtracting the averaged signal

$$h_{j+1}(t) = h_j(t) - M_{Avg_j}(t);$$

2.7 If  $h_{j+1}$  satisfies the conditions of an IMF

$$IMF_k(t) = h_{j+1}(t); \text{ the } k^{th} \text{ IMF}$$

If not

$$j = j + 1;$$

returns to 2.2

3  $r_k(t) = x(t) - IMF_k(t)$ ;

4 If  $r_{k+1}(t)$  has an extrema

$$r(t) = r_{k+1}(t); \text{ the residue}$$

And

$$x(t) = \sum_{i=1}^k IMF_i(t) + r(t) \quad (4)$$

If not

$$k = k + 1;$$

returns in 2;

end

### B. Dual-Tree Complex Wavelet Transform (DTCWT)

The DT-CWT is a proposal that tries to solve the disadvantages of real wavelets. Before going into detail on this type of algorithm, a review of the complex Wavelets will be made, for this a quick analysis of the Fourier Transformation is taken as a starting point [16]:

- The magnitude of the Fourier Transform does not oscillate positively and negatively but rather provides a positive and flat response on the Fourier domain.
- The magnitude of the Fourier Transform is totally invariant with displacements, with a simple linear phase correction that encodes displacement.
- Fourier coefficients do not suffer from aliasing and do not require a complicated property for cancellation of this when reconstructing the signal.
- The sinusoids of the multi-dimensional Fourier base are highly directional plane waves.

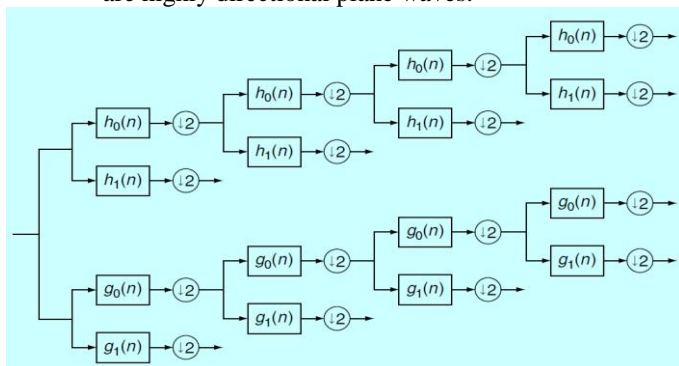


Figure 4: The functioning of dual tree [16]

The difference is mainly that the Fourier Transform is based on oscillating and complex value sinusoids, while the DWT is based on real and oscillating Wavelets. The cosine and sine oscillatory components (real and imaginary parts, respectively) form a pair of the Hilbert Transform, and in turn have a 90° separation from each other. Together they

establish an analytical signal  $e^{j\omega t}$  that is sustained only by means of a frequency axis ( $\omega > 0$ ) reducing aliasing.

Extending the concept of the Hilbert Transform slightly, it is important to say that the magnitude response of this transform is unitary for all frequencies, both positive and negative and its phase response is +90° for negative frequencies and -90° for positive frequencies (Equations (5) and (6)).

$$g'(t) = \frac{1}{\pi} \int_{-\infty}^{\infty} \frac{g(\tau)}{t-\tau} dt \quad (5)$$

$$H(f) = -j \text{sgn}(f) \quad (6)$$

From the above, the initial idea is to think of a complex wavelet transformation, which contains both a scaling function and a complex wavelet function (Equation (7)).

$$\psi_c(t) = \psi_r(t) + j\psi_i(t) \quad (7)$$

Here,  $\psi_r(t)$  would be real and even and  $\psi_i(t)$  is imaginary and odd. Moreover, if  $\psi_r(t)$  and  $\psi_i(t)$  form a pair of the Hilbert Transform, then  $\psi_c(t)$  is an analytical signal, which is only supported on the middle axis of the frequency [17].

### C. Fitness Function

The calculation of spectral evenness is finished by partitioning the geometric mean of the power spectrum by the arithmetic mean of the power spectrum, i.e.:

$$Flatness = \frac{\sqrt[N]{\prod_{n=0}^{N-1} x(n)}}{\frac{\sum_{n=0}^{N-1} x(n)}{N}} = \frac{\exp\left(\frac{1}{N} \sum_{n=0}^{N-1} \ln x(n)\right)}{\frac{1}{N} \sum_{n=0}^{N-1} x(n)} \quad (8)$$

The  $x(n)$  denotes the magnitude of binary number  $n$ .

GWO algorithm will evaluate the optimal threshold according to following fitness function.

$$Er = \min(1 - Flatness) \quad (9)$$

After spectral subtraction, filtered IMFs are summed up to get the reconstructed signal.

### D. Grey Wolf Optimization (GWO)

The GWO algorithm was proposed by Mirjalili et al. [18]. Figure 5 shows the grey wolves hierarchy. The best solution in mathematical representation of social hierarchy of wolves while assembling GWO is considered to be alpha ' $\alpha$ '. The 2<sup>nd</sup> and the 3<sup>rd</sup> best solutions are ' $\beta$ ' and ' $\delta$ ' respectively. The hunting decisions are taken by  $\alpha$ ,  $\beta$  and  $\delta$  wolves whereas ' $\omega$ ' (omega) wolves obey above 3wolves. Figure 6 depicts the possible hunting locations and encircling behaviour of wolves.

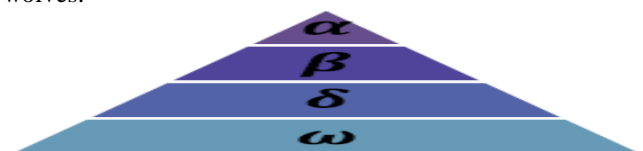


Figure 5: Grey Wolf Hierarchy[18]

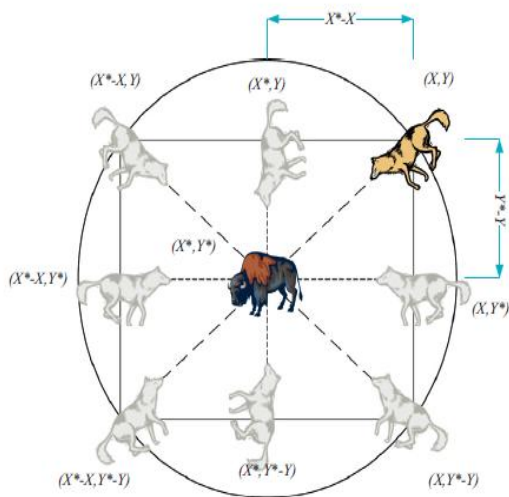


Figure 6: Possible hunting locations and encircling behaviour of wolves [18]

The encircling behaviour of the wolves around its prey can be represented as:

$$\vec{D} = |\vec{C} \cdot \vec{X}_p t - \vec{X}(t)| \quad (10)$$

$$\vec{X}(t+1) = \vec{X}_p t - \vec{A} \cdot \vec{D} \quad (11)$$

Where,  $X$  is the position vector of the wolf.  $A$  and  $C$  are coefficient vectors,  $t$  is the current iteration.

### 1. GWO Algorithm

1. Grey wolves wander in search of its prey depending on the alpha, beta and delta positions. They go away (divergence) from each other in search of a prey and gather again (convergence) while attacking the prey [19]. This divergence can be mathematically given by  $A$  and convergence is represented by  $C$ .

$$\vec{A} = 2 \cdot \vec{a} \cdot \vec{r}_1 - \vec{a} \quad (12)$$

$$\vec{C} = 2 \cdot \vec{r}_2 \quad (13)$$

Where,  $\vec{r}_1$  and  $\vec{r}_2$  are random vectors:

2. The initialization of GWO population is given by at counter iteration  $t=0$ :

$$X_i = (1, 2, 3 \dots \dots \dots n) \quad (14)$$

3. Further  $A$ ,  $C$  and  $a$  are also initialized
4. Now the fitness function for each searching agent is evaluated and is represented as:

$X_\alpha$  denotes best searching agent

$X_\beta$  denotes 2<sup>nd</sup> best searching agent

$X_\delta$  denotes 3<sup>rd</sup> best searching agent

5. If the total no. of iterations is given as  $t = n$ , then

For  $(t = 1; t \leq n)$

Using above equations update the position of searching agents

End for

6. Update  $A$  and  $C$  coefficients
7. Evaluate fitness function for each searching agent
8. Update  $X_\alpha, X_\beta, X_\delta$
9. Set  $t = t + 1$  (iteration counter increasing)
10. Return best solution  $X_\alpha$

### 2. GWO Working

1. The GWO resolves the optimization problem by generating the best solutions available during iterations.
2. The encircling behaviour gives an idea about the neighbouring circle around the solution which could be further extended into sphere (as shown in Figure 7).
3.  $A$  and  $C$  coefficient vectors help solutions to have random radii hyperspheres.
4. The hunting behaviour permits the solution to define the exact location of the prey.
5. Values of  $a$  and  $A$  are responsible for exploitation and exploration.
6. If the value of  $A$  decrease, then total number of iterations are equally divided and assigned for exploitation and exploration respectively.

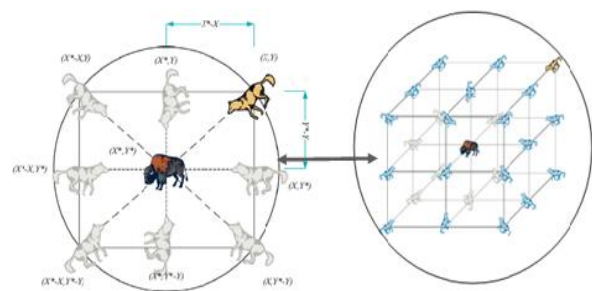


Figure 7: Extension of encircling shape into sphere

### E. Power Spectral Subtraction

The power spectral subtraction for noisy signal corrupted by AWGN is

$$E\{|Y(e^{j\omega})|^2\} = E\{|X(e^{j\omega})|^2\} + E\{|N(e^{j\omega})|^2\}$$

Or

$$E\{|X(e^{j\omega})|^2\} = E\{|Y(e^{j\omega})|^2\} - E\{|N(e^{j\omega})|^2\} \quad (13)$$

Where,  $E\{\cos(\Delta\theta)\} = 0$ .

After spectral subtraction, filtered IMFs are summed up to get the reconstructed signal.

## III. SIMULATION RESULTS

### A. Evaluation Parameters

Table 1 presents the evaluation parameters of the proposed ECG denoising method, where  $S(n)$  and  $\hat{S}(n)$  symbolize the clean and reconstructed ECG signal respectively.

Table 1: Evaluation parameters

SNR	$\frac{P_{signal}}{P_{Noise}} \text{ dB}$
PSNR	$20 \log_{10} \left[ \frac{\max\{S(n)\}}{\sqrt{\frac{1}{N} \sum_{n=1}^N  S(n) - \hat{S}(n) ^2}} \right] \text{ dB}$
MSE	$\frac{\sum_{n=1}^N [S(n) - \hat{S}(n)]^2}{\sum_{n=1}^N [S(n)]^2}$
MAE	$\frac{\sum_{n=1}^N  S(n) - \hat{S}(n) }{N}$
Cross Correlation	$r_{s(n)\hat{s}(n)}(j) = \frac{1}{N} \sum_{n=0}^{N-1} S(n)\hat{S}(n+j)$

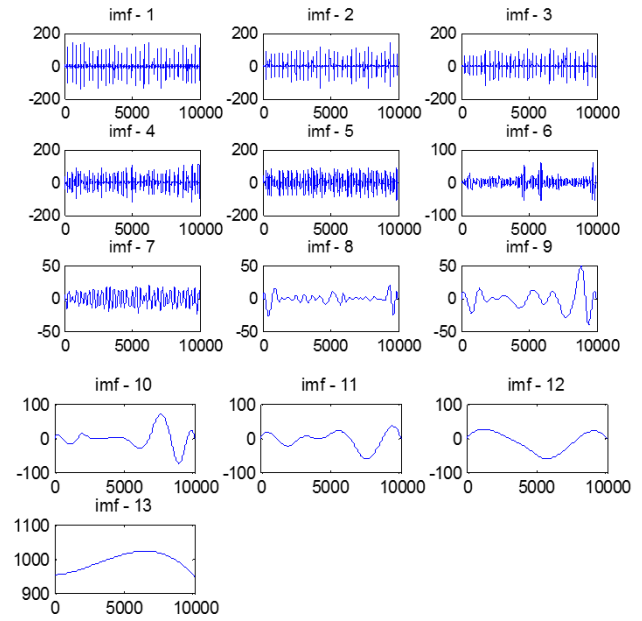


Figure 7: EMD decomposed IMFs

B. SIMULATION RESULTS

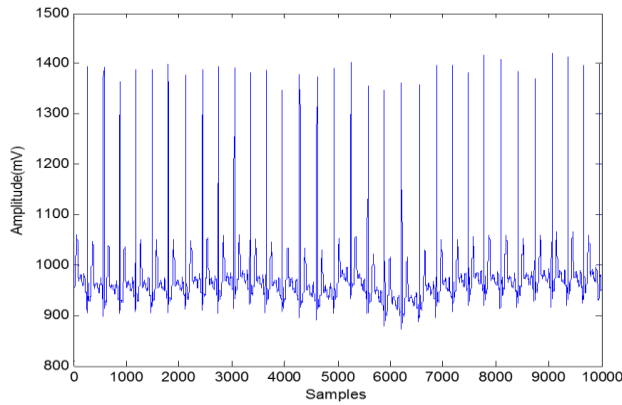


Figure 5: Original ECG signal

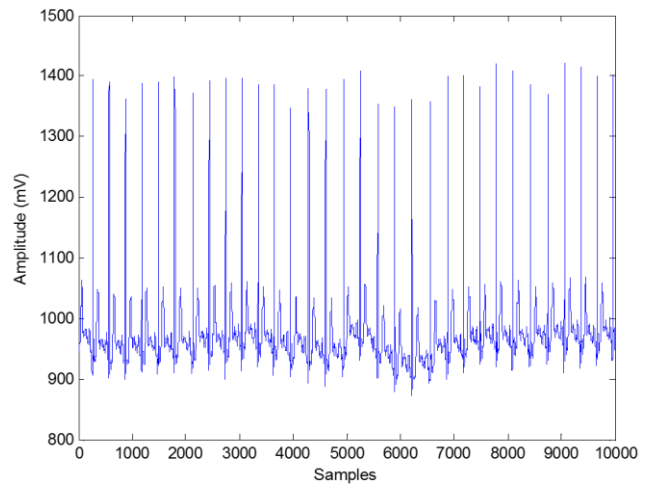


Figure 8: Signal with denoising effect

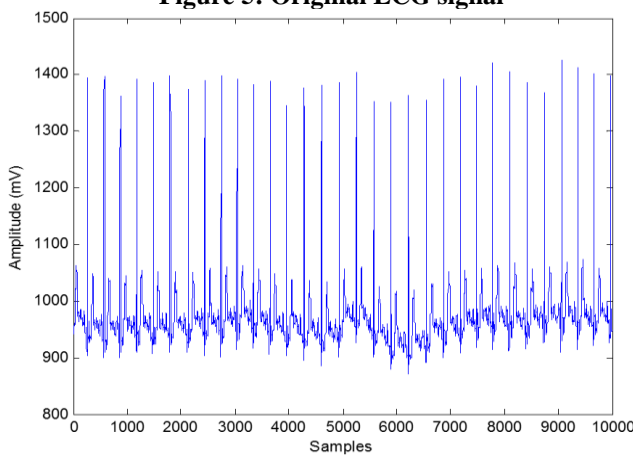


Figure 6: Signal with AWGN noise at 25 dB SNR

Table 2: Comparative analysis of results at different noise strengths

Parameters	At 6 dB Noise Strength	At 18 dB Noise Strength	At 24 dB Noise Strength
Mean Squared Error	513.216067	34.324329	7.193856
Mean Absolute Error	18.064058	4.639513	2.125187
Signal-to-Noise Ratio	32.695445 dB	44.442426 dB	51.228829 dB
Peak Signal-to-Noise Ratio	35.954989 dB	47.701971 dB	54.488374 dB
Cross Correlation	0.942410	0.995799	0.999116

**Table 4: Comparative analysis of SNR values of proposed with other two techniques for various ECG record of MIT-BIH database**

SNR (dB)	EMD (dB)	EMD-DTCWT (dB)	EMD-DTCWT-GWO (dB)
6	26.9874	30.6243	32.417
8	29.114	32.3794	34.954
10	31.146	34.4324	36.227
12	33.967	37.0514	38.7681
14	35.8421	39.3725	41.1732
16	37.5438	41.6738	43.9984
18	40.019	43.0149	44.6127

Table 3 and Table 4 represent the relative study of various methods proposed and it was found that the proposed EMD+DTCWT+GWO gives better performance against varying SNR compared to other traditional approaches.

ECG signal Record No.	SNR (dB)		
	EMD	EMD-DTCWT	EMD-DTCWT-GWO
100	40.019	43.0149	44.6127
103	41.1087	42.9027	45.3172
104	42.1873	44.0039	46.2574
116	41.6958	42.7468	44.3793
119	40.5431	44.0658	44.3619
123	41.9311	43.5738	44.2845
147	41.6734	42.9852	45.1153
203	40.4084	42.4655	45.0245
209	41.3458	43.3662	45.7163
231	42.2387	43.9734	46.0448

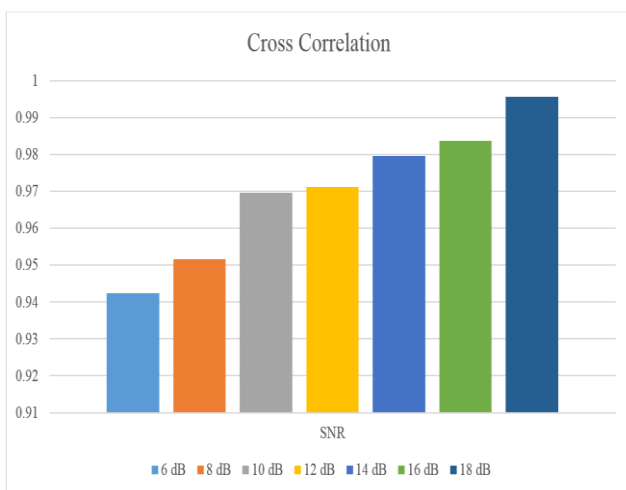


**Figure 9: Bar graph for cross correlation value under different SNR (6-18 dB) in MIT-BIH data**

Around 2-3 dB gain is attained in proposed approach. Thus the cross correlation is used as a measurement of denoising impact on ECG based on varying SNR. The cross correlation value lies between 0 to 1 using the normalization of input ECG signal. The correlation coefficient value near to 1 resemble nearest match to the reference signal. At 18 dB SNR, Figure 9 shows the maximum cross correlation compared to lower order SNR value.



**Figure 10: Bar graph for Mean Absolute Error calculation under different SNR (6-18 dB) in MIT-BIH data**

Figure 10 shows the mean absolute error according to varying SNR. It was found that the MAE value is high when noise power is more, gradually it is decreasing according to decrement in noise power. At 18 dB minimum MAE is achieved i.e. 4.6395.

#### IV. CONCLUSION

The result of work on this subject was the execution of a denoising technique which is based on the statistical properties of the DTCWT of the ECG signal. Some parameters of the suggested approach have been verified to decide the optimal choice of these in order to have the best results. The purpose of the tests carried out is to get as close as possible to the real conditions for which such treatment must work. In this framework, we deliberate the impact of denoising for low noise signals for which we added artificially generated noise. Denoising methods are necessary for the minimization of white Gaussian noise in our case. Because denoising generally enters the preprocessing phase of any acquisition or transmission chain. The simulation results were very interesting and showed the effectiveness of these methods for such an application.

#### REFERENCES

- Ghodake, Sanjay, Shashikant Ghumbre, and Sachin Deshmukh. "Electrocardiogram Signal Denoising Using Hybrid Filtering for Cardiovascular Diseases Prediction." In *Techno-Societal 2018*, pp. 271-278. Springer, Cham, 2020.
- Jenkal, Wissam, Rachid Latif, Ahmed Toumanari, Azzedine Dliou, Oussama El B'charri, and Fadel MR Maoulainine. "An efficient algorithm of ECG signal denoising using the adaptive dual threshold filter and the discrete wavelet transform." *Biocybernetics and Biomedical Engineering* 36, no. 3 (2016): 499-508.
- Qian, Chunqiang, Honghong Su, and Helong Yu. "Local means denoising of ECG signal." *Biomedical Signal Processing and Control* 53 (2019): 101571.
- Hao, Huaqing, Ming Liu, Peng Xiong, Haiman Du, Hong Zhang, Feng Lin, Zengguang Hou, and Xiuling Liu. "Multi-lead model-based ECG signal denoising by guided filter." *Engineering Applications of Artificial Intelligence* 79 (2019): 34-44.
- Wang, Ze, Feng Wan, Chi Man Wong, and Liming Zhang. "Adaptive Fourier decomposition based ECG denoising." *Computers in Biology and Medicine* 77 (2016): 195-205.
- Alyasseri, Zaid Abdi Alkareem, Ahmad Tajudin Khader, Mohammed Azmi Al-Betar, and Mohammed A. Awadallah. "Hybridizing  $\beta$ -hill climbing with wavelet transform for denoising ECG signals." *Information Sciences* 429 (2018): 229-246.

7. Shridhar, Sameera, YepugantiKaruna, SarithaSaladi, and Ramachandra Reddy. "Denoising of ECG signals using wavelet transform and principal component analysis." *Available at SSRN 3356368* (2019).
8. Singh, Omkar, and Ramesh Kumar Sunkaria. "ECG signal denoising via empirical wavelet transform." *Australasian physical & engineering sciences in medicine* 40, no. 1 (2017): 219-229.
9. Han, G., B. Lin, and Z. Xu. "Electrocardiogram signal denoising based on empirical mode decomposition technique: an overview." *Journal of Instrumentation* 12, no. 03 (2017): P03010.
10. Rakshit, Manas, and Susmita Das. "An efficient ECG denoising methodology using empirical mode decomposition and adaptive switching mean filter." *Biomedical Signal Processing and Control* 40 (2018): 140-148.
11. Kumar, Shailesh, DamodarPanigrahy, and P. K. Sahu. "Denoising of Electrocardiogram (ECG) signal by using empirical mode decomposition (EMD) with non-local mean (NLM) technique." *Biocybernetics and Biomedical Engineering* 38, no. 2 (2018): 297-312.
12. Flandrin, Patrick, Gabriel Rilling, and Paulo Goncalves. "Empirical mode decomposition as a filter bank." *IEEE signal processing letters* 11, no. 2 (2004): 112-114.
13. Rilling, Gabriel, Patrick Flandrin, and Paulo Goncalves. "On empirical mode decomposition and its algorithms." In *IEEE-EURASIP workshop on nonlinear signal and image processing*, vol. 3, no. 3, pp. 8-11. NSIP-03, Grado (I), 2003.
14. Garnaik, Sarmila, Nikhilesh Chandra Rout, and KabirajSethi. "Noise Reduction in Electrocardiogram Signal Using Hybrid Methods of Empirical Mode Decomposition with Wavelet Transform and Non-local Means Algorithm." In *Computational Intelligence in Data Mining*, pp. 639-648. Springer, Singapore, 2019.
15. Han, G., B. Lin, and Z. Xu. "Electrocardiogram signal denoising based on empirical mode decomposition technique: an overview." *Journal of Instrumentation* 12, no. 03 (2017): P03010.
16. El B'charri, Oussama, RachidLatif, KhalifaElmansouri, AbdenbiAbenaou, and WissamJenkal. "ECG signal performance de-noising assessment based on threshold tuning of dual-tree wavelet transform." *Biomedical engineering online* 16, no. 1 (2017): 26.
17. Prashar, Navdeep, MeenakshiSood, and Shruti Jain. "Dual-tree complex wavelet transform technique-based optimal threshold tuning system to deliver denoised ECG signal." *Transactions of the Institute of Measurement and Control* (2020): 0142331219895708.
18. SeyedaliMirjalili, Seyed Mohammad Mirjalili and Andrew Lewis, "Grey Wolf Optimizer", *Advances in Engineering Software*, 2014.
19. Ahmed F. Ali, "Grey Wolf Optimizer Algorithm", Scientific Research Group in Egypt, December 2014.

## AUTHORS PROFILE



**Deepak H. A.**, has received the B.E., degree in Telecommunication Engineering from VTU, Belagavi, Karnataka, India in 2007 and M.tech., degree in VLSI Design and Embedded systems from VTU, Belagavi, Karnataka, India in 2010. He has 10 years of experience in teaching and working as an Assistant Professor in the Department of Electronics and

Communication Engineering, Navkis College of Engineering, Hassan, Karnataka. Presently doing Ph.D, in the field of Signal Processing in VTU. He has published 4 research papers in National and International Journals.



**Dr. Vijayakumar T.**, working as a Professor in the department of Electronics and Communication Engineering at S J B Institute of Technology, Bangalore. He obtained B.E (Electronics and Communication), M.E (Digital Communication) degrees from the Bangalore University and Phd (VLSI and Image Processing) from Kuvempu

University. He has served as a Lecturer, Assistant Professor, Associate Professor and Professor. He has a total teaching experience of 27 years. He has served as a B.O.E for Visvesvaraya Technological University. He has published papers in National and International Journals.